Dynamical Mountain Meteorology

Dr. Yuh-Lang Lin, ylin@cat.edu; http://mesolab.org
Department of Physics/Department of Energy & Environmental Systems
North Carolina A&T State University
(Ref.: *Mesoscale Dynamics*, Y.-L. Lin, Cambridge, 2007)

Chapter 7 Flow over Two-Dimensional Mountains

(Based on Sec. 5.1 & 5.2, "Mesoscale Dynamics" by Y.-L. Lin 2007, Cambridge U. Press)

- Many well-known weather phenomena are directly related to flow over orography, such as

  - mountain waves
  - lee waves and clouds
  - rotors and rotor clouds
  - severe downslope windstorms
  - lee vortices
  - lee cyclogenesis
  - frontal distortion across mountains
  - cold-air damming
  - track deflection of midlatitude and tropical cyclones
  - coastally trapped disturbances
  - orographically induced rain and flash flooding
  - orographically influenced storm tracks.

- A majority of these phenomena are mesocale and are induced by stably stratified flow over orography. Thus, understanding the dynamics associated with stably stratified flow over a

mesoscale mountain is essential in improving the understanding of the above mentioned phenomena.

- In addition, understanding the dynamics of orographically forced flow will also help on different aspects of meteorology, such as turbulence which affect aviation safety, wind-damage risk assessment, pollution dispersion in complex terrain, and subgrid-scale parameterization of mountain wave drag in general circulation models.

5.1 Two-Dimensional Flow over Sinusoidal Mountains

[ref: 5.1 of Lin (2007)]

- Some fundamental properties of flow responses to orographic forcing can be understood by considering a two-dimensional, steady-state, adiabatic, inviscid, nonrotating, Boussinesq fluid flow over a small-amplitude mountain.

- For a two-dimensional, steady-state, adiabatic, inviscid, nonrotating, Boussinesq fluid flow, the linear governing equations (2.2.14) - (2.2.18)

$$\frac{\partial u'}{\partial t}+U\frac{\partial u'}{\partial x}+V\frac{\partial u'}{\partial y}+U_z w'-fv'+\frac{1}{\overline{\rho}}\frac{\partial p'}{\partial x}=0 \quad (2.2.14)$$

,

$$\frac{\partial v'}{\partial t}+U\frac{\partial v'}{\partial x}+V\frac{\partial v'}{\partial y}+V_z w'+fu'+\frac{1}{\overline{\rho}}\frac{\partial p'}{\partial y}=0, \quad (2.2.15)$$

$$\frac{\partial w'}{\partial t}+U\frac{\partial w'}{\partial x}+V\frac{\partial w'}{\partial y}-g\frac{\theta'}{\overline{\theta}}+\frac{1}{\overline{\rho}}\frac{\partial p'}{\partial z}+\frac{p'}{\overline{\rho}H}=0, \quad (2.2.16)$$

$$\frac{1}{c_s^2}\left(\frac{\partial p'}{\partial t}+U\frac{\partial p'}{\partial x}+V\frac{\partial p'}{\partial y}\right)-\frac{\overline{\rho}}{H}w'+\overline{\rho}\nabla\cdot\boldsymbol{V}'=\frac{\overline{\rho}}{c_p\overline{T}}q', \tag{2.2.17}$$

$$\frac{\partial\theta'}{\partial t}+U\frac{\partial\theta'}{\partial x}+V\frac{\partial\theta'}{\partial y}+\frac{N^2\overline{\theta}}{g}w'=\frac{\overline{\theta}}{c_p\overline{T}}q', \tag{2.2.18}$$

can be simplified to

$$U\frac{\partial u'}{\partial x}+U_z w'+\frac{1}{\rho_o}\frac{\partial p'}{\partial x}=0, \tag{5.1.1}$$

$$U\frac{\partial w'}{\partial x}-g\frac{\theta'}{\theta_o}+\frac{1}{\rho_o}\frac{\partial p'}{\partial z}=0, \tag{5.1.2}$$

$$\frac{\partial u'}{\partial x}+\frac{\partial w'}{\partial z}=0, \tag{5.1.3}$$

$$U\frac{\partial\theta'}{\partial x}+\frac{N^2\theta_o}{g}w'=0. \tag{5.1.4}$$

- The above set of equations can be further reduced to *Scorer's equation* (1954),

$$\nabla^2 w'+l^2(z)w'=0, \tag{5.1.5}$$

where $\nabla^2=\partial^2/\partial x^2+\partial^2/\partial z^2$ is the two-dimensional Laplacian operator, and l is the Boussinesq form of the *Scorer parameter* (Scorer 1949), which is defined as:

$$l^2(z)=\frac{N^2}{U^2}-\frac{U_{zz}}{U}. \tag{5.1.6}$$

Equation (5.1.5) serves as a central tool for numerous theoretical studies of small-amplitude, two-dimensional mountain waves.

It may also be interpreted as a vorticity equation upon being multiplied by U (Smith 1979).

- The first term, $U(w'_{xx} + w'_{zz})$, is the rate of change of vorticity following a fluid particle.

- The second term, $N^2 w'/U$, is the rate of vorticity production by buoyancy forces.

- The last term, $-U_{zz} w'$, represents the rate of vorticity production by the redistribution of the background vorticity (U_z).

In the extreme case of very small Scorer parameter, i.e. very weak stratification and/or basic wind has zero or constant shear, (5.1.5) reduces to the irrotational or potential flow [i.e., no vorticity production by buoyancy forces, $N^2 w'/U$ - the 2nd term of (5.1.5)]

$$\nabla^2 w' = 0 . \qquad (5.1.7)$$

As discussed in Chapter 3 [(3.5.22)], the buoyancy force is negligible in this extreme case. If the forcing is symmetric in

the basic flow direction, such as a cylinder in an unbounded fluid or a bell-shaped mountain in a half-plane, then the flow is symmetric. For this particular case, there is no drag produced on the mountain since the fluid is inviscid.

- In order to simplify the mathematics of the steady state mountain wave problem, one may assume that $U(z)$ and $N(z)$ are independent of height, and a sinusoidal mountain

$$h(x) = h_m \sin kx \,, \tag{5.1.8}$$

where h_m is the mountain height and k is the wave number of the terrain.

For an inviscid fluid flow, the lower boundary condition requires the fluid particles to follow the mountain, so that the streamline slope equals the terrain slope locally,

$$\frac{w}{u} = \frac{w'}{U + u'} = \frac{dh}{dx} \quad \text{at} \quad z = h(x)\,. \tag{5.1.9}$$

- For a small-amplitude mountain, this leads to the linear lower boundary condition

$$w' = U\frac{dh}{dx} \quad \text{at} \quad z = 0\,. \tag{5.1.10}$$

or

$$w'(x,0) = U\, h_m k \cos kx \quad \text{at} \quad z = 0, \tag{5.1.11}$$

for flow over a sinusoidal mountain as described by (5.1.8).

Due to the sinusoidal nature of the forcing, it is natural to look for solutions in terms of sinusoidal functions,

$$w'(x,z) = w_1(z)\cos kx + w_2(z)\sin kx\,. \tag{5.1.12}$$

Substituting the above solution into (5.1.5) with a constant Scorer parameter leads to

$$w_{izz} + (l^2 - k^2)w_i = 0, \quad i = 1,2\,. \tag{5.1.13}$$

As discussed in Chapter 3 [(3.5.7)], two cases are possible: (a) $l^2 < k^2$ and (b) $l^2 > k^2$.

- Case 1: $N/U < k$ or $Na/U < 2\pi$, where a is the terrain wavelength.

Physically, this means that the basic flow has relatively weaker stability and stronger wind, or that the mountain is narrower than a certain threshold.

For example, to satisfy the criterion for a flow with U = 10 ms^{-1} and N = 0.01 s^{-1}, the wavelength of the mountain should be smaller than 6.3 km.

In fact, this criterion can be rewritten as $(a/U)/(2\pi/N)<1$. The numerator, a/U, represents the advection time of an air parcel passing over one wavelength of the terrain, while the denominator, $2\pi/N$, represents the period of buoyancy oscillation due to stratification.

This means that the time an air parcel takes to pass over the terrain is less than it takes for vertical oscillation due to buoyancy force. In other words, buoyancy force plays a smaller role than the horizontal advection.

In this situation, (5.1.13) can be rewritten as

$$w_{izz}-(k^2-l^2)w_i=0, \quad i=1,2. \tag{5.1.14}$$

The solutions of the above second-order differential equation with constant coefficient may be obtained

$$w_i = A_i e^{\lambda z} + B_i e^{-\lambda z}, \quad i = 1, 2, \tag{5.1.15}$$

where

$$\lambda = \sqrt{k^2 - l^2}\,. \tag{5.1.16}$$

Similar to that described in Section 3.4, the upper boundedness condition requires $A_i = 0$ because the energy source is located at $z = 0$.

Applying the lower boundary condition, (5.1.11), and the upper boundary condition ($A_i = 0$) to (5.1.15) yields

$$B_1 = U\, h_m k; \quad B_2 = 0\,. \tag{5.1.17}$$

This gives the solution,

$$w'(x,z) = w_1(z)\cos kx = U h_m k e^{-\sqrt{k^2 - l^2}\, z} \cos kx\,, \tag{5.1.18}$$

The vertical displacement (η) is defined as $w' = D\eta / Dt$ which reduces to

$$w' = \frac{D\eta}{Dt} = U\frac{\partial \eta}{\partial x} \tag{5.1.19}$$

for a steady-state flow.

Equation (5.1.18) can then be expressed in terms of η,

$$\eta = \frac{1}{U}\int_0^x w'\,dx = h_m \sin kx\, e^{-\sqrt{k^2-l^2}\,z} \,. \qquad (5.1.20)$$

The above solution is sketched in Fig. 5.1a.

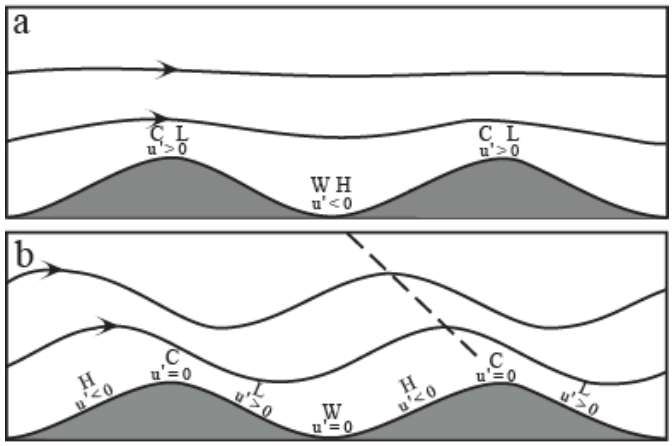

Fig. 5.1: The steady-state, inviscid flow over a two-dimensional sinusoidal mountain when (a) $l^2 < k^2$ (or $N < kU$), where k is the terrain wavenumber ($= 2\pi/a$, where a is the terrain wavelength), or (b) $l^2 > k^2$ (or $N > kU$). The dashed line in (b) denotes the constant phase line which tilts upstream with height. The maxima and minima of u', p' (H and L), and θ' (W and C) are also denoted in the figures.

The disturbance is symmetric with respect to the vertical axis and decays exponentially with height. Thus, the flow belongs to the evanescent flow regime as discussed in Section 3.5.

The buoyancy force plays a minor role compared to that of the advection effect. The other variables can also be obtained by using the governing equations and (5.1.18),

$$u' = U\, h_m \sqrt{k^2 - l^2}\, \sin kx\, e^{-\sqrt{k^2 - l^2}\, z}, \tag{5.1.21}$$

$$p' = -\rho_o U^2\, h_m \sqrt{k^2 - l^2}\, \sin kx\, e^{-\sqrt{k^2 - l^2}\, z}, \tag{5.1.22}$$

$$\theta' = -(\theta_o N^2 / g)\, h_m \sin kx\, e^{-\sqrt{k^2 - l^2}\, z}. \tag{5.1.23}$$

The maxima and minima of u', p', and θ' are also denoted in Fig. 5.1a.

- The coldest (warmest) air is produced at the mountain peak (valley) due to adiabatic cooling (warming).
- The flow accelerates over the mountain peaks and decelerates over the valleys.
- From the horizontal momentum equation, (5.1.1) with $U_z = 0$, or (5.1.22), a low (high) pressure is produced over the mountain peak (valley) where maximum (minimum) wind is produced.

Note that (5.1.1) is also equivalent to the *Bernoulli equation*, which states that the pressure perturbation is out of phase with the horizontal velocity perturbation.

Since no pressure difference exists between the upslope and downslope, this flow produces no net wave drag on the mountain (mountain drag).

The *mountain drag* can be computed either from the horizontal pressure force on the mountain over a wavelength,

$$D = \frac{k}{2\pi}\int_{-\pi/k}^{\pi/k} p'(x, z=0)\left(\frac{dh}{dx}\right)dx\,, \tag{5.1.24}$$

or equivalently, as the negative of the vertical flux of horizontal momentum (*momentum flux*) in the wave motion,

$$\mathcal{D} = -\frac{\rho_o k}{2\pi}\int_{-\pi/k}^{\pi/k} u'w'\,dx\,. \tag{5.1.25}$$

Note that the *Eliassen and Palm's theorem*, (4.4.10),

[Additional reading] Quote from Ch.4 (Lin 2007):

$$F = \rho_o\int_{-\infty}^{\infty} u'w'\,dx = constant\,, \quad \text{when } U \neq 0\,. \tag{4.4.9}$$

This is the *Eliassen and Palm* (1960) *theorem*, which states that the vertical flux of horizontal momentum does not change with height except possibly at levels where $U = 0$ or in the layer of forcing. If the integration of (4.4.8) is taken over one horizontal wavelength, we have

$$\overline{p'w'} = -\rho_o U\overline{u'w'}\,. \tag{4.4.10}$$

Thus, the vertical flux of wave energy is negatively proportional to the vertical flux of horizontal momentum if $U > 0$. For an energy source located in the lower troposphere, such as a mountain, the momentum flux is downward because the energy flux is upward.

indicates that the vertical flux of horizontal momentum in a steady-state flow is negatively proportional to the vertical energy flux, $\overline{p'w'}$ (where the overbar denotes the average over a wavelength).

➢ Case 2: $l^2 > k^2$ ($N/U > k$ or $Na/U > 2\pi$)

As discussed in Section 3.5, this means that the basic flow has relatively stronger stability and weaker wind or that the mountain is wider.

For example, and as mentioned earlier, to satisfy the criterion for a flow with U = 10 ms^{-1}and N = 0.01 s^{-1}, the terrain wavelength should be larger than 6.3 km. Since $(a/U)/(2\pi/N) > 1$, the advection time is larger than the period of the vertical oscillation.

In other words, buoyancy force plays a more dominant role than the horizontal advection.

In this case, (5.1.13) can be written as

$$w_{izz} + m^2 w_i = 0\,, \quad m^2 = l^2 - k^2, \quad i = 1, 2\,. \tag{5.1.26}$$

We look for solutions in the form

$$w_i(z) = A_i \sin mz + B_i \cos mz, \;\; i = 1, 2 \,. \tag{5.1.27}$$

Substituting (5.1.27) into (5.1.12) leads to

$$\begin{aligned} w'(x,z) = {} & C\cos(kx+mz) + D\sin(kx+mz) + \\ & E\cos(kx-mz) + F\sin(kx-mz). \end{aligned} \tag{5.1.28}$$

In the above equation, terms of (*kx*+*mz*) have an upstream phase tilt with height, while terms of (*kx*-*mz*) have a downstream phase tilt.

It can be shown that terms of $(kx+mz)$ have a positive *vertical energy flux* and should be retained since the energy source in this case is located at the mountain surface. This satisfies the Sommerfeld radiation boundary condition (Sommerfeld 1949), as discussed in Section 4.4 (HW5). Thus, the solution requires $E = F = 0$.

This flow regime is characterized as the upward propagating wave regime, as discussed in Chapter 3. As in the first case, the lower boundary condition requires

$$C = Uh_m k, \quad D = 0 \,. \tag{5.1.29}$$

This leads to

$$w'(x,z) = Uh_m k \cos(kx+mz) \,. \tag{5.1.30}$$

Other variables can be obtained through definitions or the governing equations,

$$\eta(x,z) = h_m \sin(kx + mz), \tag{5.1.31}$$

$$u'(x,z) = -Uh_m m \cos(kx + mz), \tag{5.1.32}$$

$$p'(x,z) = \rho_o U^2 h_m m \cos(kx + mz), \text{ and} \tag{5.1.33}$$

$$\theta'(x,z) = -\frac{N^2 \theta_o h_m}{g} \sin(kx + mz). \tag{5.1.34}$$

The vertical displacement of the flow, and the maxima and minina of u', p', and θ' are depicted in Fig. 5.1b.

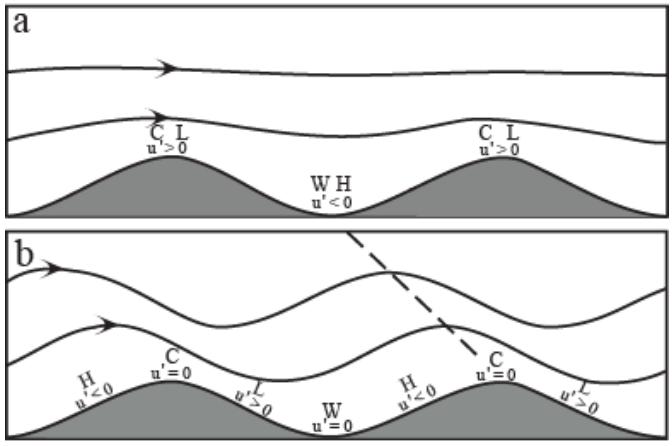

Fig. 5.1: The steady-state, inviscid flow over a two-dimensional sinusoidal mountain when (a) $l^2 < k^2$ (or $N < kU$), where k is the terrain wavenumber ($= 2\pi / a$, where a is the terrain wavelength), or (b) $l^2 > k^2$ (or $N > kU$). The dashed line in (b) denotes the constant phase line which tilts upstream with height. The maxima and minima of u', p' (H and L), and θ' (W and C) are also denoted in the figures.

Note that the flow pattern is no longer symmetric. The constant phase lines are tilted upstream (to the left) with height, thus producing a high pressure on the windward slope and a low

pressure on the lee slope. Based on (5.1.32) or the Bernoulli equation (5.1.1), the flow decelerates over the windward slope and accelerates over the lee slope. The coldest and warmest spots are still located over the mountain peaks and valleys, respectively. The mountain drag can be calculated either from (5.1.24) or (5.1.25)

$$D = \frac{k}{2\pi}\int_{-\pi/k}^{\pi/k} p'(x, z=0)\left(\frac{dh}{dx}\right)dx\,, \tag{5.1.24}$$

$$\mathcal{D} = -\frac{\rho_o k}{2\pi}\int_{-\pi/k}^{\pi/k} u'w'dx\,. \tag{5.1.25}$$

to be

$$D = \frac{1}{2}\rho_o U^2 h_m^2 k\sqrt{l^2 - k^2}\,. \tag{5.1.35}$$

The positive wave drag on the mountain is produced by the high pressure on the windward slope and the low pressure on the lee slope. This also can be understood through (5.1.25) and the out-of-phase relationship of u' and w' over the windward and lee slopes, as shown in Fig. 5.1b.

➢ Extreme Case: $l^2 >> k^2$

This means that buoyancy effect dominates and the advection effect is totally negligible.

In other words, the vertical pressure gradient force and the buoyancy force are roughly in balance and the vertical acceleration can be ignored.

Thus, the mountain waves become hydrostatic. In this limiting case, the governing equation becomes

$$w'_{zz}+l^2w'=0\,. \tag{5.1.36}$$

The flow pattern repeats itself in the vertical with a wavelength of $\lambda_z = 2\pi/l = 2\pi U/N$, which is also referred to as the hydrostatic vertical wavelength.

The regime boundary between the regimes of vertically propagating waves and evanescent waves can be found by letting $l = k$, which leads to $a = 2\pi U/N$.

The relation among the mountain waves discussed in this subsection is sketched in Fig. 5.2.

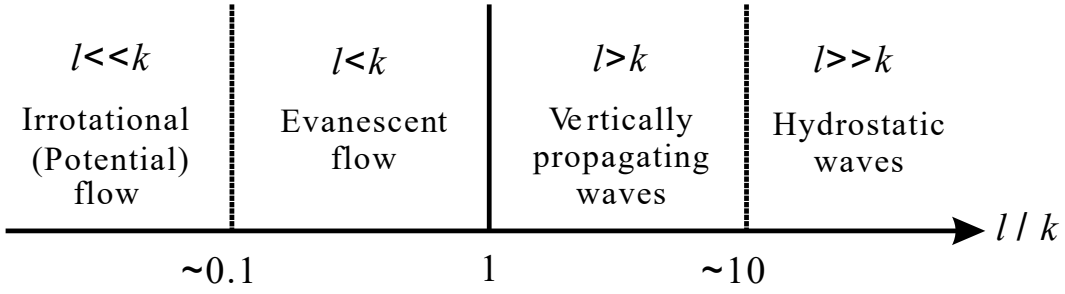

Fig. 5.2: Relations among different mountain wave regimes as determined by l/k, where l is the Scorer parameter and k is the wave number.

5.2 Two-Dimensional Flow over Isolated Mountains

(5.2 Flows over two-dimensional isolated mountains – Lin 2007)
(Classical equation editor: $c_p \neq f(k)$)

5.2.1 Uniform basic flow

The mountain wave problem in Section 5.1 may be extended to be more realistic by assuming an isolated mountain.

Taking the one-sided Fourier transform (Appendix 5.1) of (5.1.5)

$$\nabla^2 w' + l^2(z) w' = 0, \tag{5.1.5}$$

where $\nabla^2 = \partial^2/\partial x^2 + \partial^2/\partial z^2$ and

$$l^2(z) = \frac{N^2}{U^2} - \frac{U_{zz}}{U}. \tag{5.1.6}$$

[Note that $l^2 = N^2/U^2$ is constant for a uniform flow, as assumed in Sec. 5.2.1]

Appendix 5.1: Some mathematical techniques and relations

(a) Fourier Transform

The Fourier transform of $f(x)$ is defined as

$$\hat{f}(k) = \frac{1}{2\pi}\int_{-\infty}^{\infty} f(x)\, e^{-ikx} dx \quad \text{and} \tag{A5.1.1a}$$

$$f(x) = \int_{-\infty}^{\infty} \hat{f}(k)\, e^{ikx} dk. \tag{A5.1.1b}$$

One of the advantages of the Fourier transform is that it can distinguish the upward- and downward propagation of wave energy.

An alternative Fourier transform pair may be defined as

$$\hat{f}(k) = \frac{1}{2\pi}\int_{-\infty}^{\infty} f(x)\, e^{-ikx} dx \quad \text{and} \tag{A5.1.2a}$$

$$f(x) = 2\,\mathrm{Re}\int_0^\infty \hat{f}(k)\, e^{ikx} dk\,, \qquad \text{(A5.1.2b)}$$

for real function *f*. This is also called the one-sided Fourier transform (Queney et al. 1960).

Occasionally, the following pair of Fourier transform has been adopted in the literature,

$$\hat{f}(k) = \frac{1}{\pi}\int_{-\infty}^\infty f(x)\, e^{-ikx} dx \quad \text{and} \qquad \text{(A5.1.3a)}$$

$$f(x) = \mathrm{Re}\int_0^\infty \hat{f}(k)\, e^{ikx} dk \,. \qquad \text{(A5.1.3b)}$$

Other variations of Fourier transform pairs, such as using e^{ikx} (e^{-ikx}) in the forward (inverse or backward) Fourier transform, have also been used in the literature. No matter which form of the Fourier transform is used, the Fourier transform pair should be able to transform the original function back to itself after performing the forward and inverse transforms.

Fourier transform is useful in helping solve differential equations. For example, see http://www.physics.ucf.edu/~schellin/teaching/phz3113/lec9-3.pdf

It yields

$$\hat{w}_{zz} + (l^2 - k^2)\hat{w} = 0\,. \qquad (5.2.1)$$

The Fourier transform of the linear lower boundary condition (homework), (5.1.10), is

$$\hat{w}(k, z=0) = ikU\,\hat{h}(k)\,. \qquad (5.2.2)$$

For constant Scorer parameter, the solution of (5.2.1) can be written into two parts,

$$\hat{w}(k,z) = \hat{w}(k,0)\, e^{i\sqrt{l^2-k^2}\,z} \quad \text{for} \quad l^2 > k^2 \quad \text{and} \qquad (5.2.3a)$$

$$\hat{w}(k,z) = \hat{w}(k,0)\, e^{-\sqrt{k^2-l^2}\,z} \quad \text{for} \quad l^2 < k^2\,. \qquad (5.2.3b)$$

Taking the inverse one-sided Fourier transform (Appendix 5.1)

A reminder: The *one-sided Fourier transform* pair is defined as

$$\hat{f}(k) = \frac{1}{2\pi}\int_{-\infty}^{\infty} f(x)\, e^{-ikx}\, dx \qquad \text{(A5.1.2a)}$$

$$f(x) = 2\,\mathrm{Re}\int_{0}^{\infty} \hat{f}(k)\, e^{ikx}\, dk \qquad \text{(A5.1.2b)}$$

of (5.2.3) yields the solution in the physical space,

$$w'(x,z) = 2\,\mathrm{Re}\left[\int_0^l ikU\ \hat{h}(k)\ e^{i\sqrt{l^2-k^2}\,z} e^{ikx}\, dk + \int_l^{\infty} ikU\ \hat{h}(k)\ e^{-\sqrt{k^2-l^2}\,z} e^{ikx}\, dk\right], \qquad (5.2.4)$$

where Re represents the real part.

The first integration on the right hand side of (5.2.4) represents the upward propagating wave which satisfies the upper radiation boundary condition, while the second integration represents the evanescent wave which satisfies the boundedness upper boundary condition.

Note that (5.2.4) is for a continuous spectrum of Fourier modes, instead of just one single mode as considered in Sec. 5.1.

For simplicity, let us consider a bell-shaped mountain or the *Witch of Agnesi* mountain profile,

$$h(x) = \frac{h_m a^2}{x^2 + a^2}, \qquad (5.2.5)$$

where h_m is the mountain height and a is the half-width where the mountain height is $h_m/2$.

The advantage of using a bell-shaped mountain lies in that its one-sided Fourier transform (Appendix 5.1)

Again, the one-sided Fourier transform pair is defined as

$$\hat{f}(k) = \frac{1}{2\pi}\int_{-\infty}^{\infty} f(x)\, e^{-ikx}\, dx \quad \text{and}$$

$$f(x) = 2\,\mathrm{Re}\int_0^{\infty} \hat{f}(k)\, e^{ikx}\, dk\,,$$

is in a simple form,

$$\hat{h}(k) = \frac{h_m a}{2} e^{-ka}, \quad \text{for } k > 0. \tag{5.2.6}$$

The Fourier transform for any k is $(h_m a/2)\exp(-|k|a)$. (10/7/14)

Case 1: $l^2 << k^2$ (i.e., $al << 1$ or $Na << U$)

Note that for bell-shaped mountains, we assume $k \approx 1/a$, instead of $k = 2\pi/a$ for sinusoidal mountains.

As discussed earlier, the flow becomes a potential flow in which the buoyancy plays a negligible role. In this case, (5.2.4)

$$w'(x,z) = 2\,\mathrm{Re}\left[\int_0^l ikU\ \hat{h}(k)\ e^{i\sqrt{l^2-k^2}z} e^{ikx} dk + \int_l^{\infty} ikU\ \hat{h}(k)\ e^{-\sqrt{k^2-l^2}z} e^{ikx} dk\right], \tag{5.2.4}$$

can be approximated by

$$w'(x,z) \approx 2\,\mathrm{Re}\left[U\int_0^\infty ik\,\hat{h}(k)\,e^{-kz}e^{ikx}dk\right] = 2\,\mathrm{Re}\left[U\int_0^\infty ik\left(\frac{h_m a}{2}\right)e^{-ka}\,e^{-kz}e^{ikx}dk\right]. \tag{5.2.7}$$

Since $w' = U\partial\eta/\partial x$, the Fourier transform of η can be obtained from that of $\hat{w}$,

$$\hat{\eta}(k,z) = \frac{\hat{w}(k,z)}{ikU}. \tag{5.2.8}$$

Substituting (5.2.7) into (5.2.8) leads to

$$\eta(x,z) = h_m a\,\mathrm{Re}\int_0^\infty e^{-k(z+a-ix)}dk = \frac{h_m a(z+a)}{x^2+(z+a)^2}. \tag{5.2.9}$$

Therefore, similar to the sinusoidal mountain case, the flow pattern is symmetric with respect to the center of the mountain ridge ($x=0$). However, the amplitude decreases with height linearly, instead of exponentially. The flow pattern is depicted in Fig. 5.3a.

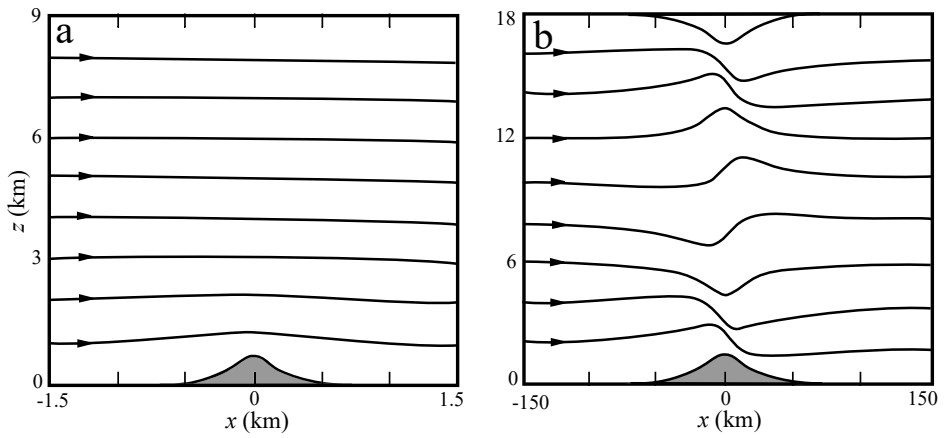

Fig. 5.3: Streamlines of steady state flow over an isolated, bell-shaped mountain when (a) $l^2 << k^2$ (or $Na << U$), where a is the half-width of the mountain, or (b) $l^2 >> k^2$ (or $Na >> U$). (Lin 2007; Adapted after Durran 1990)

Case 2: $l^2 >> k^2$ (i.e., $al >> 1$ or $Na >> U$)

As discussed in the previous section, the vertical acceleration due to the buoyancy force plays a dominant role.

In this case, the solution (5.2.4)

$$w'(x,z) = 2\,\mathrm{Re}\left[\int_0^l ikU\,\hat{h}(k)\,e^{i\sqrt{l^2-k^2}z}e^{ikx}dk + \int_l^\infty ikU\,\hat{h}(k)\,e^{-\sqrt{k^2-l^2}z}e^{ikx}dk\right], \tag{5.2.4}$$

can be approximated by

$$w'(x,z) \approx 2\,\mathrm{Re}\left[U\int_0^\infty ik\hat{h}(k)e^{ilz}e^{ikx}dk\right] = 2\,\mathrm{Re}\left[U\int_0^\infty ik\left(\frac{h_m a}{2}\right)e^{-ka}e^{ilz}e^{ikx}dk\right]. \tag{5.2.10}$$

Similarly, the vertical displacement can be obtained,

$$\eta(x,z) = 2\,\mathrm{Re}\int_0^\infty \frac{h_m a}{2} e^{-ka} e^{i(kx+lz)} dk == \frac{h_m a(a\cos lz - x\sin lz)}{x^2 + a^2} . \qquad (5.2.11)$$

This type of flow is characterized as a hydrostatic mountain wave.

The disturbance confines itself over the mountain in horizontal, but repeats itself in vertical with a wavelength of $2\pi U / N$.

Without the Boussinesq approximation, the above solution becomes

$$\eta(x,z) = \left(\frac{\rho_s}{\rho(z)}\right)^{1/2} \left[\frac{h_m a(a\cos lz - x\sin lz)}{x^2 + a^2}\right], \qquad (5.2.12)$$

where ρ_s is the air density near surface.

Equation (5.2.12) indicates that the wave amplitude will increase with a decreased air density of the basic flow. That is, the wave amplitude will increase at higher altitudes since air density decreases with height in a stably stratified flow.

This helps explain the wave amplification in the higher atmosphere, such as large-amplitude gravity waves in the stratosphere, which causes aviation turbulence leading to aviation hazards.

As described in the previous section, other fields can be obtained by the governing equations, (5.1.1)-(5.1.4) with $U_z = 0$ (no basic wind shear).

The wave drag on the mountain surface in this hydrostatic limit can be obtained by applying the *Parseval theorem* (Appendix 5.1),

$$D = \int_{-\infty}^{\infty} p'(x, z=0)\frac{dh}{dx}dx = \int_{-\infty}^{\infty} p'(x,0)\frac{dh^*}{dx}dx = \frac{\pi}{4}\rho_o U N h_m^2, \tag{5.2.13}$$

where h^* is the complex conjugate of h. The momentum is transferred to a level where the wave breaks down, which is not included in the linear theory.

Case 3: $l^2 \approx k^2$ (i.e., $al \approx 1$ or $Na \approx U$)

An asymptotic solution can be obtained for this case. In this case, all terms of the vertical momentum equation, (5.1.2) are equally important. Both asymptotic methods and numerical methods have been applied to solve the problem.

In the following, we apply the *stationary phase method* to this particular problem. We look for solutions far downstream, $x \to \infty$ in (5.2.4). In this limit, the second term on the right side of (5.2.4)

$$w'(x,z) = 2\,\mathrm{Re}\left[\int_0^l ikU\ \hat{h}(k)\ e^{i\sqrt{l^2-k^2}z}e^{ikx}dk + \int_l^{\infty} ikU\ \hat{h}(k)\ e^{-\sqrt{k^2-l^2}z}e^{ikx}dk\right],$$

approaches 0 due to fast oscillation of $\exp(ikx)$, according to the *Riemann-Lebesgue Lemma* (Appendix 5.1).

> ***(c) Riemann–Lebesgue Lemma***
>
> $$\lim_{x\to\infty}\int_{-\infty}^{\infty}\hat{f}(k)e^{ikx}dk = 0 \quad \text{if} \quad \hat{f}(k) \text{ is smooth.} \qquad \text{(A5.1.5)}$$
>
> A smooth function here means that the function is ordinary and absolutely integrable. The above conclusion is reached by the reasoning of cancellation.

Thus, for large x, we have

$$\eta(x,z) \approx 2\,\mathrm{Re}\int_0^l \hat{h}(k)e^{i\phi(k)}dk\,, \qquad (5.2.14)$$

where

$$\phi(k) = \sqrt{l^2 - k^2}\,z + kx \qquad (5.2.15)$$

is a *phase function*. Based on the stationary phase method, we will look for a particular k^* such that

$$\frac{d\phi}{dk} = 0 \quad \text{at} \quad k = k^*\,, \qquad (5.2.16)$$

where k^* is called the point of stationary phase.

With large x or z, $\exp(i\phi)$ will oscillate rapidly and, therefore, η will approach 0, according to Riemann-Lebesgue Lemma.

However, near k^*, the contribution to the integration by $\exp(i\phi)$ still remains because ϕ is approximately constant.

Substituting the phase function (5.2.15) into (5.2.16) leads to the *influence function*,

$$\frac{z}{x} = \frac{\sqrt{l^2 - k^{*2}}}{k^*}, \tag{5.2.17}$$

in the region near k^*.

Taking the *Taylor's series expansion* of $\phi(k)$ near k^* gives

$$\phi(k) = \phi(k^*) + \left[\frac{\partial \phi}{\partial k}\right]_{k^*} \tilde{k} + \frac{1}{2!}\frac{\partial^2 \phi}{\partial k^2}\tilde{k}^2 + \ldots, \tag{5.2.18}$$

where $\tilde{k} = k - k^*$.

The second term on the right side of the above equation disappears due to the definition of k^* in (5.2.16). Thus, (5.2.14) becomes

$$\eta(x,z) = 2\,\mathrm{Re}\left[\hat{h}(k^*)e^{i\phi(k^*)}\int_0^l e^{i\phi_{kk}\tilde{k}^2/2}dk\right]. \tag{5.2.19}$$

For a bell-shaped mountain,

$$\eta(x,z) = \sqrt{2\pi}\; h_m a e^{-k^* a}\left[\frac{(l^2 - k^{*2})^{3/4}}{lz^{1/2}}\right]\cos\left(\sqrt{l^2 - k^{*2}}\,z + k^* x - \frac{\pi}{4}\right), \tag{5.2.20}$$

where

$$k^* = \frac{l}{\sqrt{(z/x)^2 + 1}}. \qquad (5.2.21)$$

Figure 5.4 shows an example of a flow over a ridge of intermediate width ($l^2 \approx k^2$) where the buoyancy force is important, but not so dominant that the flow becomes hydrostatic. The nearly periodic waves located to the upper right of the mountain are the *dispersive tail* of nonhydrostatic waves with k less than, but not much less than l.

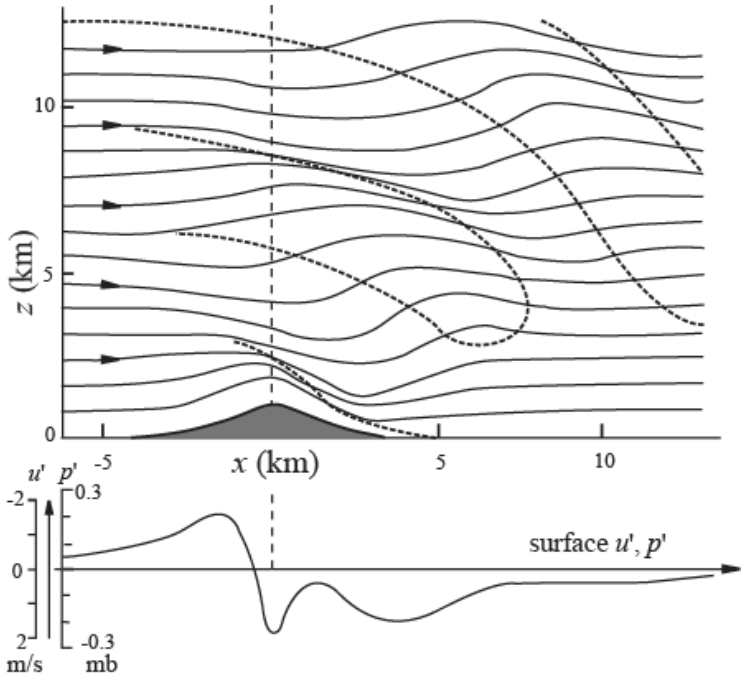

Fig. 5.4: Flow over a two-dimensional ridge of intermediate width ($l^2 \approx k^2$, or $al = Na/U = 1$) where the buoyancy force is important, but not so dominant that the flow is hydrostatic. The zero phase lines are denoted by dotted curves. The waves on the lee aloft are the *dispersive tail* of the nonhydrostatic waves ($k < l$, but not $k << l$). The flow and orographic parameters are: U = 10 ms^{-1}, N = 0.01 s^{-1}, h_m = 1 km, and a = 1 km. (Lin 2007; Adapted after Queney 1948)

In fact, the influence function, (5.2.17), is related to the energy propagation associated with the mountain waves. The group velocity (c_{gm}) in the frame of reference fixed with the mountain can be obtained from (3.5.11),

Eq. (3.5.11)

$$\Omega = \frac{\pm Nk}{\sqrt{k^2 + m^2}}$$

$$\boldsymbol{c}_{gm} = \left(U + \frac{\partial \omega}{\partial k} \right) \boldsymbol{i} + \frac{\partial \omega}{\partial m} \boldsymbol{k}, \tag{5.2.22}$$

where m in gm stands for mountain and

$$\omega = \frac{-Nk}{\sqrt{k^2 + m^2}}. \tag{5.2.23}$$

Substituting (5.2.23) into (5.2.22) leads to

$$\boldsymbol{c}_{gm} = U\boldsymbol{i} + \boldsymbol{c}_{ga} = \left[U - \frac{Nm^2}{(k^2 + m^2)^{3/2}} \right] \boldsymbol{i} + \left[\frac{Nkm}{(k^2 + m^2)^{3/2}} \right] \boldsymbol{k}, \tag{5.2.24}$$

where $\boldsymbol{c}_{ga}$ is the group velocity relative to the air.

Furthermore, the requirement of stationary waves, $c_{px} + U = 0$, implies

$$U = \frac{N}{\sqrt{k^2 + m^2}}. \tag{5.2.25}$$

In (5.2.23), the negative sign is chosen in order to obtain positive c_{gz} by assuming positive k and m due to the use of one-sided Fourier transform.

The relationship among $c_{px}\boldsymbol{i}$, $\boldsymbol{c}_{gm}$ and $\boldsymbol{c}_{ga}$ is sketched in Fig. 5.5.

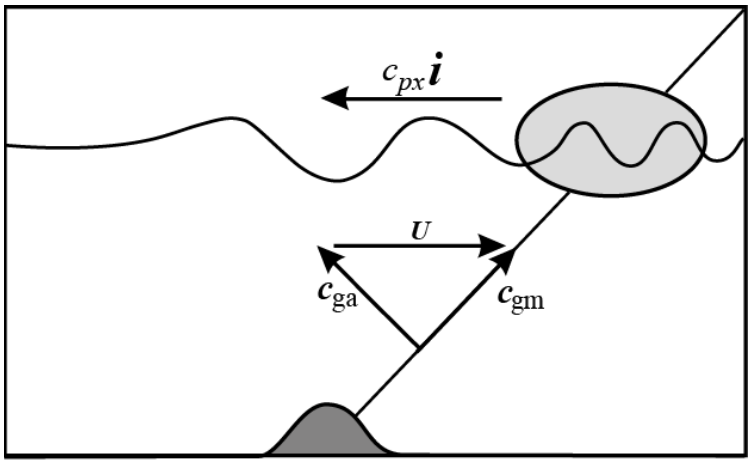

Fig. 5.5: A schematic illustrating the relationship among the group velocity with respect to (w.r.t) to the air ($\boldsymbol{c}_{\mathrm{ga}}$), group velocity w.r.t. to the mountain ($\boldsymbol{c}_{\mathrm{gm}}$), horizontal phase speed ($c_{px}\boldsymbol{i}$) and the basic wind. The horizontal phase speed of the wave is exactly equal and opposite to the basic wind speed. The wave energy propagates upward and upstream relative to the air, but is advected downstream by the basic wind. The energy associated with the mountain waves propagates upward and downstream relative to the mountain. (Lin 2007; After Smith 1979, reproduced with the permission from Elsvier.)

The upstream phase speed of the mountain wave is exactly equal to and opposite of the basic wind speed. The wave energy propagates upward and upstream relative to the air, but is advected downstream by the basic wind.

Thus, relative to the mountain, the energy associated with the mountain waves propagates upward and downstream. The slope of the group velocity can be obtained by substituting U of (5.2.25) into (5.2.24) and then calculating the slope,

$$\frac{c_{gz}}{c_{gx}} = \frac{m}{k} = \sqrt{\frac{N^2}{U^2 k^2} - 1} = \frac{\sqrt{l^2 - k^2}}{k} = \frac{z}{x}. \qquad (5.2.26)$$

In deriving the second equality, we have used (5.2.25), while in deriving the last equality, we have used (5.2.17) near the *point of stationary phase*, i.e. $k = k^*$.

Therefore, the point of stationary phase is the value of k corresponding to a wave with a group velocity beam as shown in Fig. 5.5. Waves are found downstream since the horizontal group velocity is less than the phase speed.

For general cases, such as $l^2 < k^2$ or $l^2 > k^2$, it is not easy to obtain analytical solutions from (5.2.4). With the advancement of numerical techniques, such as the Fast Fourier Transform (FFT) and computers, solutions can be approximately obtained numerically with the implementation of proper boundary conditions.

5.2.2 Basic flow with variable Scorer parameter

In the real atmosphere, the basic wind and stratification normally vary with height. To study the mountain waves produced by this type of basic flow, we assume that the Scorer parameter, (5.1.6), is a slowly-varying function of z .

In this situation, we expect to find a solution of (5.2.1)

$$\hat{w}_{zz} + (l^2 - k^2)\hat{w} = 0. \quad (5.2.1)$$

in form of,

$$\hat{w}(k,z) = \mathcal{A}(k,z)\, e^{i\phi(k,z)}, \qquad (5.2.27)$$

where $\mathcal{A}(k,z)$ is a slowly varying amplitude function, and $\phi(k,z)$ is the slow-varying phase function. Substituting (5.2.27) into (5.2.1) yields

$$\left[-\mathcal{A}\phi_z^2 + (l^2 - k^2)\mathcal{A}\right] + i(\mathcal{A}\phi_{zz} + 2\mathcal{A}_z\phi_z) + \mathcal{A}_{zz} = 0. \qquad (5.2.28)$$

The last term makes a minor contribution and can be neglected, since $A(k,z)$ is a slow-varying function of z. Thus, the above equation reduces to

$$\phi_z = \sqrt{l^2 - k^2}\ , \text{ and} \qquad (5.2.29)$$

$$\frac{\partial}{\partial z}(\mathcal{A}^2\phi_z) = 0 . \qquad (5.2.30)$$

Combining the above two equations leads to

$$\mathcal{A}^2\sqrt{l^2 - k^2} = constant . \qquad (5.2.31)$$

For long (hydrostatic) waves ($l^2 >> k^2$), the above equation reduces to

$$\mathcal{A}^2 l = constant . \qquad (5.2.32)$$

This implies that the amplitude of the vertical velocity increases (decreases) significantly in regions of weak (strong) stratification or strong (weak) wind.

For example, the mountain wave tends to steepen when it propagates to the region below a jet stream or a jet streak since the basic wind speed increases there.

Note that in applying (5.2.27) to solve the problem, and in neglecting the last term of (5.2.28), we have implicitly adopted a first-order WKBJ approximation.

A second-order WKBJ approximation has been used to calculate wind profile effects on mountain wave drag (e.g., Teixeira and Miranda 2006). It is necessary to extend the WKBJ approximation to second order for these effects to be taken into account.

Based on (5.2.32) and previous discussions, waves may amplify in certain layers due to: (a) weaker stratification, (b) stronger wind, such as a jet stream or jet streak, (c) nonlinear steepening, and (d) abrupt decrease in the mean density, leading to an increase of $\sqrt{\rho_s / \rho(z)}$, in (5.2.12). 10/15/14

5.2.3 Trapped lee waves

One of the most prominent features of mountain waves is the long train of wave clouds over the lee of mountain ridges in the lower atmosphere, such as those shown in Fig. 5.6.

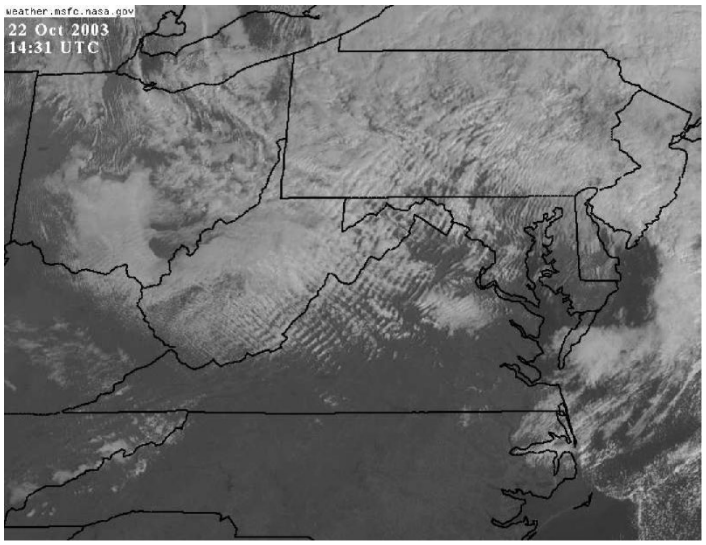

Fig. 5.6: Satellite imagery for lee wave clouds observed at 1431 UTC, 22 October 2003, over western Virginia. Clouds originate at the Appalachian Mountains. (Courtesy of NASA)

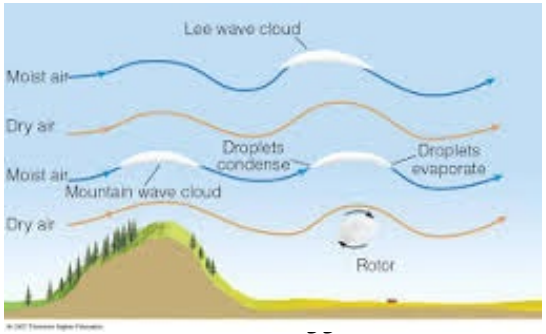

A schematic for lee waves and rotors

More pictures:
http://images.google.com/images?hl=en&q=lee+waves&um=1&ie=UTF-8&ei=dB-yS4f0OIWClAeF26HtBA&sa=X&oi=image_result_group&ct=title&resnum=4&ved=0CDYQsAQwAw

This type of wave differs from the dispersive tails in Fig. 5.4 in that it is located in the lower atmosphere and there is no vertical phase tilt.

It will be shown below that this type of trapped lee waves, or resonance waves, occurs when the Scorer parameter decreases rapidly with height (Scorer 1949).

The dynamics of trapped lee waves may be understood by considering a two-layer stratified fluid system. The wave equations for the vertical displacement in Fourier space may be written in a form similar to (5.2.1),

$$\hat{w}_{zz} + (l^2 - k^2)\hat{w} = 0 . \quad (5.2.1)$$

$$\hat{\eta}_{zz} + [l_1^2 - k^2]\hat{\eta} = 0 \quad \text{for} \quad -H \le z < 0 \ \text{and} \qquad (5.2.33a)$$

$$\hat{\eta}_{zz} - [k^2 - l_2^2]\hat{\eta} = 0 \quad \text{for} \quad 0 \le z . \qquad (5.2.33b)$$

In this two-layer fluid system, we have assumed that $l_2^2 < k^2 < l_1^2$.

For convenience, the ground and the interface of the lower and upper layers are assumed to be located at $z = -H$ and $z = 0$, respectively.

The free wave solutions may be written as

$$\hat{\eta}_1(k,z) = C\left[\cos\mu z - \frac{\lambda}{\mu}\sin\mu z\right] \text{ and} \qquad (5.2.34a)$$

$$\hat{\eta}_2(k,z) = C\, e^{-\lambda z}, \qquad (5.2.34b)$$

where $\mu = \sqrt{l_1^2 - k^2}$, $\lambda = \sqrt{k^2 - l_2^2}$ and C is a constant coefficient to be determined by the lower boundary condition.

The boundedness upper boundary condition has been applied to exclude the $\exp(\lambda z)$ term, and the kinematic and dynamic boundary conditions at the interface, i.e. the continuities of $\hat{w}$ and $\hat{w}_z$ at $z = 0$, have also been applied.

In order to obtain a complete solution of the boundary value problem for a specific obstacle, we may apply the linear lower boundary condition,

$$\hat{\eta}_1(k,-H) = \hat{h}(k). \qquad (5.2.38)$$

Substituting the above equation into (5.2.34) and taking the inverse Fourier transform of $\hat{\eta}(k,z)$ leads to the forced wave solution in the lower layer,

$$\eta_1(x,z) = 2\,\mathrm{Re}\int_0^\infty \frac{\hat{h}(k)(\cos\mu z - (\lambda/\mu)\sin\mu z)e^{ikx}}{(\cos\mu H + (\lambda/\mu)\sin\mu H)}dk\,. \qquad (5.2.39)$$

The singularity in the denominator of the above equation corresponds to the resonance mode that will produce lee waves.

Equation (5.2.39) can be solved asymptotically or numerically with a given mountain-shape function (Scorer 1949; Smith 1979). Without enforcing a lower boundary condition, (5.2.34) represents free waves associated with this two-layer fluid system.

The resonance waves are obtained by seeking the zeros of (5.2.34a) with $z = -H$,

$$\cot\mu H = -\lambda/\mu\,. \qquad (5.2.35)$$

The resonance wave number (k_r^*) may be obtained by solving the above equation either numerically or graphically.

The criterion for the existence of one or more resonance waves may be obtained (Scorer 1949):

$$l_1^2 - l_2^2 \geq \frac{\pi^2}{4H^2}\,. \qquad (5.2.36)$$

A more general criterion for resonance waves of the *n*th mode is

$$\left[\frac{(2n+1)\pi}{2H}\right]^2 \geq (l_1^2 - l_2^2) \geq \left[\frac{(2n-1)\pi}{2H}\right]^2 . \qquad (5.2.37)$$

The above criterion implies that *in order to have resonance (lee) waves, the Scorer parameter in the lower layer must be much greater than that in the upper layer*.

In other words, the lower layer must be more stable or with a much slower basic wind speed than the upper layer.

Figure 5.7 shows lee waves simulated by a nonlinear numerical model for two-layer airflow over a bell-shaped mountain. Due to the co-existence of the upward propagating waves and downward propagating waves, there exists no phase tilt in the lee waves.

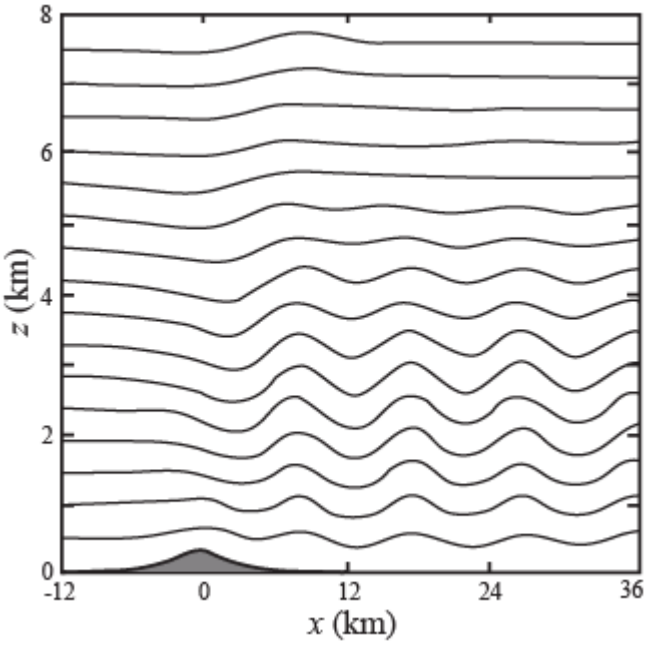

Fig. 5.7: Lee waves simulated by a nonlinear numerical model for a two-layer airflow over a bell-shaped mountain. Displayed are the quasi-steady state streamlines. In the lower layer (below 5 km approximately), $l^2 = 9x10^{-7}\,\mathrm{m}^{-2}$, while in the upper layer, $l^2 = 2x10^{-7}\,\mathrm{m}^{-2}$. (Lin 2007; Adapted after Durran 1986b)

Once lee waves form, regions of reversed cross-mountain winds near the surface beneath the crests of the lee waves may develop due to the presence of a reversed pressure gradient force.

In the presence of surface friction, a sheet of vorticity parallel to the mountain range forms along the lee slopes, which originates in the region of high shear within the boundary layer.

The vortex sheet separates from the surface, ascends into the crest of the first lee wave, and remains aloft as it is advected downstream by the undulating flow in the lee waves (Doyle and Durran 2004).

The vortex with recirculated air is known as *rotor* and the process that forms it is known as *boundary layer separation*, which will be further discussed in subsection 5.4.2 along with lee vortices.

These rotors are often observed to the lee of steep mountain ranges such as over the Owens Valley, California, on the eastern slope of Sierra Nevada (e.g., Grubišić and Lewis 2004). Occasionally, a turbulent, altocumulus cloud forms with the rotor and is referred to as *rotor cloud*.

Some useful pictures of rotor clouds can be found at the following website:

- rotor clouds
- https://www.eol.ucar.edu/field_projects/t-rex (T-REX Field Experiment)
- http://opensky.library.ucar.edu/collections/OSGC-000-000-011-085 (T-REX mountain wave model intercomparison)

5.2.4 Bore [Lin 2007, Sec. 3.4, Figs. 3.3 & 3.4]

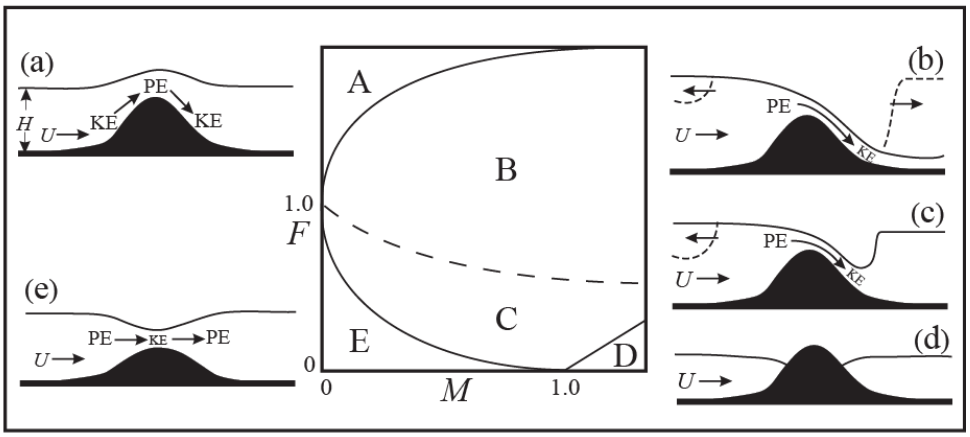

Fig. 3.3: Five flow regimes of the transient one-layer shallow water system, based on the two nondimensional control parameters ($F = U/\sqrt{gH}$, $M = h_m/H$).

(a) **Regime A**: supercritical flow
(b) **Regime B**: flow with both upstream and downstream propagating hydraulic jump
(c) **Regime C**: flow with upstream propagating jump and downstream stationary jump
(d) **Regime D**: completely blocked flow
(e) **Regime E**: subcritical flow. The dashed lines in (b) and (c) denote transient water surface. In regimes B and C, upstream flow is partially blocked. (Adapted after Baines 1995 and Durran 1990)